



저작자표시-비영리-변경금지 2.0 대한민국

이용자는 아래의 조건을 따르는 경우에 한하여 자유롭게

- 이 저작물을 복제, 배포, 전송, 전시, 공연 및 방송할 수 있습니다.

다음과 같은 조건을 따라야 합니다:



저작자표시. 귀하는 원저작자를 표시하여야 합니다.



비영리. 귀하는 이 저작물을 영리 목적으로 이용할 수 없습니다.



변경금지. 귀하는 이 저작물을 개작, 변형 또는 가공할 수 없습니다.

- 귀하는, 이 저작물의 재이용이나 배포의 경우, 이 저작물에 적용된 이용허락조건을 명확하게 나타내어야 합니다.
- 저작권자로부터 별도의 허가를 받으면 이러한 조건들은 적용되지 않습니다.

저작권법에 따른 이용자의 권리는 위의 내용에 의하여 영향을 받지 않습니다.

이것은 [이용허락규약\(Legal Code\)](#)을 이해하기 쉽게 요약한 것입니다.

[Disclaimer](#)

Master of Science

Biocompatibility of Fillers Following Application of  
Hyaluronic acid at Different Anatomic Injection Sites

The Graduate School  
Of the University of Ulsan

Department of Medical Science  
Jiyeon Kang

Biocompatibility of Fillers Following Application of  
Hyaluronic acid at Different Anatomic Injection Sites

Supervisor: Woo-Chan Son

A Dissertation

Submitted to  
the Graduate School of the University of Ulsan.

In partial Fulfillment of the Requirements  
for the Degree of

Master of Science

by

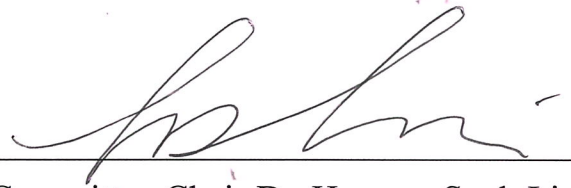
Jiyeon Kang

The Graduate School  
of the University of Ulsan  
Department of Medical Science

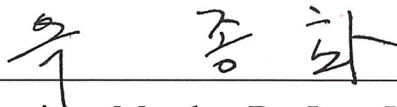
August 2023

# Biocompatibility of Fillers Following Application of Hyaluronic acid at Different Anatomic Injection Sites

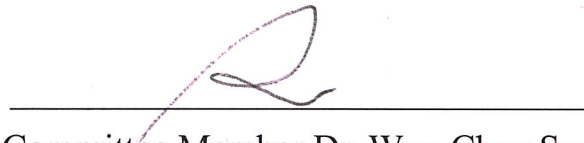
This certifies that the master's thesis of Jiyeon Kang is approved.



Committee Chair Dr. Hyeong-Seok Lim



Committee Member Dr. Jong Hoa Ok



Committee Member Dr. Woo-Chan Son

The Graduate School  
of the University of Ulsan  
Department of Medical Science  
August 2023

# Contents

<b>ABSTRACT.....</b>	<b>iii</b>
<b>LIST OF FIGURES AND TABLES .....</b>	<b>v</b>
<b>INTRODUCTION .....</b>	<b>1</b>
<b>MATERIALS AND METHODS.....</b>	<b>4</b>
1. Animal .....	4
2. Hyaluronic Acid Filler.....	4
3. Animal Model .....	4
4. Magnetic Resonance Imaging for Volumetric evaluation.....	5
5. Histopathological examination.....	5
6. Immunohistochemical staining for Inflammatory reaction .....	5
7. Histochemical and Immunohistochemical staining for Collagen synthesis.....	6
7.1. Sirius Red .....	6
7.2. Masson’s Trichrome .....	7
7.3. Immunohistochemical staining .....	7
8. Verhoeff Van Gieson staining for Elastic fiber synthesis .....	7
9. Western blot.....	7
10. Immunohistochemical staining for Vascular Distribution .....	8
11. Statistical analyses.....	8
<b>RESULTS.....</b>	<b>1 1</b>
1. Magnetic Resonance Imaging for Volumetric evaluation.....	1 1
2. Biocompatibility evaluation through Histopathological examination.....	1 3
2.1 Alcian blue.....	1 3

2.2	Hematoxylin and eosin .....	1 5
2.3	Immunohistochemical staining for CD 68 and Ly6g .....	1 6
3.	Collagen synthesis.....	1 8
3.1	Masson's Trichrome and Sirius Red .....	1 8
3.2	Immunohistochemical staining for collagen I .....	1 9
4.	Elastic fiber .....	2 1
5.	Collagen synthesis microenvironment.....	2 3
5.1	Western blot.....	2 3
5.2	Immunohistochemical staining for CD31 .....	2 5
<b>DISCUSSION.....</b>		<b>2 7</b>
<b>REFERENCES.....</b>		<b>3 1</b>
국문요약 .....		3 4

## ABSTRACT

Hyaluronic acid (HA) is an anionic glycosaminoglycan composed of repeating disaccharide units of D-gluconic acid and N-acetyl glucosamine. It is a natural polymer in living organisms that provides tissue volume and hydration. HA plays a significant role in various physiological processes such as tissue repair, morphogenesis, and cell proliferation and migration. HA promotes tissue synthesis and matrix remodeling, making it an essential component of the viscoelastic intracellular matrix that provides tissue volume and protects the skin. Its ability to bind and retain water molecules helps keep tissues hydrated and contributes to a smooth and natural appearance when used in dermal fillers.

Interactions between fibroblasts and extracellular matrix (ECM) are critical for cell function. Several studies have reported that cross-linked HA injection stimulates type I collagen by inducing fibroblast proliferation. The importance of the ECM microenvironment in regulating the active ability of fibroblasts has been emphasized. Collagen is a major structural protein that provides strength and support to tissues. Collagen synthesis by fibroblasts is regulated by the transforming growth factor-beta (TGF- $\beta$ ) pathway, which activates downstream effector proteins such as the Smad transcription factor. TGF- $\beta$  can contribute to collagen synthesis by activating the MAPK and PI3K/AKT pathways.

Biocompatibility of dermal filler is critically important as it is affected by the host tissue response and the properties of the implanted material. Interactions of implanted materials with cells induce reactions that impair the filler's long-term efficacy and safety. Therefore, proper histological evaluation is required to evaluate tissue reactions to implanted materials and to ensure safety and efficacy.

Dermal fillers, including HA fillers, are commonly used for aesthetic rejuvenation to correct fine lines, increase facial volume, and improve skin quality. Dermal fillers are applied to anatomical areas according to the purpose. The choice of anatomical site for filler injection

should consider the injected layer and the skin thickness in that area. However, thorough biocompatibility studies focused on anatomical areas have not been studied yet.

In this study, the Back and Flank of mouse were selected as representative areas of the “eyelid” and “nasal tip” in clinical based on skin thickness. Histological examination was performed to evaluate the biocompatibility of the filler and the difference in collagen synthesis according to the anatomical injection site. Then, differences in the collagen synthesis microenvironment between anatomical injection sites were compared to evaluate the suitability of the anatomical structure of the injection site according to the type of filler when introducing a new filler product for clinical use.

As a result of the MRI, it was observed that the volume increase caused by HA injection occurred more in the Flank, and collagen synthesis was observed to occur better in the Flank through immunohistochemical (IHC) staining, Masson’s trichrome and Sirius red staining. In addition, western blot and CD31 IHC were performed to evaluate the difference in the collagen synthesis microenvironment. It was observed that the Flank had a lot of subcutaneous fat, blood vessels, and active differentiation of fibroblasts. Therefore, volume increase and collagen synthesis by HA injection occurred better in the Flank with many subcutaneous fat and fibroblasts.

In this study, biocompatibility was evaluated using various evaluation methods such as radiology (MRI) and molecular biology (western blot) as well as a histological examination of filler injection. In addition, it provided insight into clinical use by selecting an anatomical area in consideration of the site suitable for the filler and comparing the difference.

**Keywords** : Hyaluronic acid (HA); Collagen synthesis; ECM microenvironment; Biocompatibility; Anatomical injection site



## LIST OF FIGURES AND TABLES

Figure 1. Volumetric evaluation HA fill <i>in vivo</i> .....	12
Figure 2. Evaluation of biodegradability of HA filler using Alcian blue .....	14
Figure 3. Inflammatory reaction over time after injection of HA.....	17
Figure 4. Collagen staining with histochemical and IHC .....	20
Figure 5. Elastic fiber staining with Verhoeff van Gieson .....	22
Figure 6. Evaluation of fibroblast differentiation with Western blot .....	24
Figure 7. Evaluation of vascular distribution and subcutaneous fat thickness .....	26
Table 1. The list of antibodies used for Immunohistochemical analysis in this study .....	10
Table 2. Antibody information used for the Immunohistochemical staining in this study .....	10

# INTRODUCTION

Hyaluronic acid (HA) is an anionic glycosaminoglycan composed of repeating disaccharide units of D-glucuronic acid and N-acetyl-glucosamine [1]. It is a naturally occurring polymer found in all living organisms. HA is significantly involved in important physiological processes such as tissue repair and morphogenesis, which involve the proliferation and migration of tissue cells [2, 3]. During these processes, tissue synthesis of HA is dramatically increased. HA promotes matrix remodeling in addition to facilitating cell migration and proliferation [4]. HA is a significant component of the viscoelastic intracellular matrix that provides and maintains adequate tissue volume and serves to protect the skin [5, 6]. Due to its ability to bind and retain water molecules, HA keeps tissues hydrated and can increase injection volume, filling the soft tissue space and producing a smooth and natural appearance [7]. HA has a stimulating effect on fibroblasts, the cells responsible for producing collagen, a protein that gives skin its structure and firmness.

Fibroblasts are cells that play a critical role in the synthesis and deposition of extracellular matrix (ECM) components, including collagen. Collagen is a major structural protein that provides strength and support to various tissues in the body. The collagen synthesis by fibroblasts is regulated by various signaling pathways, including the transforming growth factor-beta (TGF- $\beta$ ) pathway. TGF- $\beta$  is a multifunctional cytokine that can stimulate the collagen production and other ECM components [8]. TGF- $\beta$  signaling is transmitted through a transmembrane receptor complex composed of two types of serine/threonine kinase receptors known as TGF- $\beta$  type I and II receptors (T $\beta$ RI and T $\beta$ RII, respectively) [9, 10]. When TGF- $\beta$  binds to T $\beta$ RII, it activates T $\beta$ RI, phosphorylating downstream effector proteins, including Smad transcription factors. Activated Smad proteins translocate to the nucleus, where they regulate the transcription of target genes, including genes encoding collagen and other ECM components [9, 11]. In addition to Smads, TGF- $\beta$  signaling can also activate

different signaling pathways, such as the mitogen-activated protein kinase (MAPK) pathway and the phosphoinositide 3-kinase (PI3K)/Akt pathway, which can also contribute to collagen synthesis [12].

Extracellular matrix supports the epidermis and mainly comprises type I collagen fibrils synthesized by fibroblasts. Adherent cells such as fibroblasts indicate that interactions between the ECM are important for cell function. Several studies have reported that injection of cross-linked HA, an injectable space-filling material, stimulates type I collagen by inducing fibroblast proliferation. In addition, several studies emphasize the importance of the ECM microenvironment in regulating the active ability of fibroblasts [10].

Due to HA has advantages such as excellent biocompatibility, non-immunogenicity, non-carcinogenicity, and easy biodegradability, chemically modified cross-linked HA is widely used in cosmetic procedures [13].

An ideal filler material has the following characteristics: 1) Biocompatibility and stability 2) Stable at the injection site 3) Maintained volume and flexibility 4) Does not cause skin or mucosal protrusion 5) Minimal foreign body response 6) Not eliminated by phagocytosis 7) Minimal mobility 8) Does not cause foreign substance granuloma [14]. The biocompatibility of dermal filler is very important as it is affected by the host tissue response and the properties of the implanted material [15, 16]. Interactions of implanted materials with cells induce reactions that may impair the filler's long-term efficacy and safety. Minimal tissue reactivity and mobility of injected HA fillers are important characteristics for FDA safety approval [17]. Therefore, proper histological evaluation is a prerequisite for evaluating tissue response to implant materials [15].

Currently, Dermal fillers are used for aesthetic rejuvenation to correct fine lines, increase facial volume, and improve skin quality. These are applied to anatomical areas according to the purpose. The injected layer and the skin thickness along the anatomical area should be

considered for augmentation purposes [18]. However, thorough biocompatibility studies focused on anatomical area has not been studied yet.

In this study, when fillers were injected, biocompatibility was evaluated through histological examination between anatomical injection sites and differences in collagen synthesis were compared. Therefore, considering skin thickness, “eyelid” with less subcutaneous fat and “nasal tip” with more subcutaneous fat and fibrous tissue were selected as the Back and Flank of the mouse, respectively. In addition, differences in the collagen synthesis microenvironment between anatomical injection sites were compared to evaluate the suitability of the anatomical structure of the injection site according to the type of filler when introducing a new filler product for clinical use.

# MATERIALS AND METHODS

## 1. Animal

Seven-week-old female SKH1 hairless mice (n=24) purchased from Orient Bio, Inc. (Seongnam-si, Korea) were used in these experiments. Mice were housed in a specific pathogen-free facility, and in a climate-controlled room with a temperature of  $22\pm 2^{\circ}\text{C}$ , humidity  $55\pm 5\%$ , and a 12 hours dark-light cycle. All experimental procedures were approved by the Institutional Animal Care and Use Committee of Asan Medical Center (Permit Number: 2021-12-228).

## 2. Hyaluronic Acid Filler

Neuramis<sup>®</sup> VOLUME Lidocaine (Medytox Inc., Cheongju-si, Korea) was used for this study. This product has a 20 mg/ml concentration and a molecular weight of 1,000 kDa.

The filler was a mono-phasic filler, and less than 0.4 ppm of 1,4-butanediol diglycidyl ether (BDDE) was used as the cross-linking agent.

## 3. Animal Model

Inhalation anesthesia was induced in each mouse with 3% isoflurane. Neuramis<sup>®</sup> VOLUME Lidocaine was injected subcutaneously at a dose of 150 $\mu\text{L}$  in two different injection sites of the Back and Flank. The test period was set by referring to the ISO guideline “Biological evaluation of medical device – Part 6: Tests for local effects after implantation.” According to this guideline, the testing intervals should span a significant portion of the degradation time frame of the test material. It is stated that the examination period should include the following:

- An early time for evaluating initial tissue reactions.
- A middle time when tissue reactions are expected to be most pronounced.
- A late time when the minimum amount of the material remains at the injection site.

Therefore, considering the degradation rate of HA, the total test period was set at 36 weeks, and skin tissues (injection site) were sampled and analyzed after autopsy 4 times (n=6 for each time point).

#### **4. Magnetic Resonance Imaging for Volumetric evaluation**

T1 and T2-weighted images were taken *in vivo* at 0, 4, 6, 12, 24, 30, and 36 weeks at the Bioimaging Center of Asan LifeScience Research Institute located in Asan Medical Center, Seoul. The volume was calculated using the ImageJ (Version f1.52a, National Institutes of Health, MD, USA) based on the T2 axial image. The area of each slice was multiplied by the slice thickness (2 mm) to obtain the volume, and the total HA filler volume was calculated by adding the volumes of all cross-sections and then converting it into an actual ratio.

#### **5. Histopathological examination**

Skin (injection sites) tissues from each animal were harvested and fixed in 10 % neutral formalin. The tissue was trimmed, dehydrated using a Shandon Excelsior tissue processor (Thermo Fisher Scientific), penetrated with paraffin, and embedded into paraffin blocks using and EG1150H paraffin-embedding station (Leica Biosystems, Wetzlar, Germany). The paraffin block was sectioned in 3 $\mu$ m, and Hematoxylin and Eosin (H&E) staining was performed.

To evaluate the biodegradability of HA, staining was performed using Alcian Blue Stain Kit (pH 2.5, Mucin Stain) (ab150662, abcam).

#### **6. Immunohistochemical staining for Inflammatory reaction**

Immunohistochemical staining of the skin (injection sites) sections was performed using an automated slide preparation system (Benchmark XT; Ventana Medical Systems Inc., Tucson, AZ). Deparaffinization, epitope retrieval, and immunostaining were performed according to

the manufacturer's instructions with EZ Prep Concentration, Cell Conditioning Solutions and the BMK UltraView Universal DAB Detection Kit (#760-500).

Deparaffinization of the skin sections was conducted by EZ Prep (#950-102), a mild detergent solution, with heating. Epitope retrieval was performed by Tris based buffer, Cell Conditioning Solution (CC1), with a slightly basic pH. Next, the skin (injection sites) sections were stained with primary antibodies as listed in **Table 1** and **2** for 36 or 60 minutes at 37°C. UltraMap Anti-rabbit HRP (#760-4315) and UltraMap Anti-rat HRP (#760-4456) were used as a secondary antibody for 16 or 32 minutes at 37°C. Positive signals were amplified using UltraView DAB and UltraView Copper included UltraView Universal DAB Detection Kit and sections were counterstained with Hematoxylin (#760-2021) and Bluing reagents (#760-2037). Stained slides were scanned with a digital slide scanner (Motic Easy Scan Pro 6-FS, Motic Digital Pathology, SF, USA) at 40X magnification. The positive cells in the skin (injection sites) were quantified using the QuPath software (Version 0.3.0., University of Edinburgh, Edinburgh, UK).

## **7. Histochemical and Immunohistochemical staining for Collagen synthesis**

### **7.1. Sirius Red**

The Picro Sirius Red Stain Kit (ab150681, Abcam) was used to evaluate fibrotic collagen deposition according to the manufacturer's instructions. At first, deparaffinize sections and hydrate in distilled water. After deparaffinization of paraffin section slides, hydrate in distilled water. Treat with phosphomolybdic acid and incubate at room temperature for 2 minutes. Then, stain with Picro Sirius Red for 60 minutes and treat with hydrochloric acid followed by incubation at room temperature for 2 minutes. Wash three times with distilled water between each step. Finally, wash with 70% ethanol, followed by dehydration, clearing, and mounting.

## **7.2. Masson's Trichrome**

To assess the amount of fibrotic collagen deposition as collagen are synthesized in the HA filler, formalin-fixed paraffin-embedded (FFPE) blocks for the skin (injection sites) tissues were sectioned to 3  $\mu\text{m}$  thickness using a microtome (RM2255, Leica Microsystem, Wetzlar, Germany) and then stained with Masson's trichrome. Using ImageJ (Version 1.52a, National Institutes of Health, MD, USA) collagen intensity in the skin was quantified for the selected five views of a sectioned slide at 200 $\times$  magnification.

## **7.3. Immunohistochemical staining**

For identifying the expression for the collagen I proteins, immunohistochemical staining of the skin (injection sites) sections was performed using an automated slide preparation system (Benchmark XT; Ventana Medical Systems Inc., Tucson, AZ, USA). Primary antibody information and incubation time used for staining are listed in **Tables 1** and **2**.

## **8. Verhoeff Van Gieson staining for Elastic fiber synthesis**

The Verhoeff-Van Gieson Stain Kit (VB-3019, VitroVivo Biotech) evaluated elastic fiber according to the manufacturer's instructions. At first, sections are deparaffinized and hydrated in distilled water. Then treat with Verhoeff's Working Solution and incubate at room temperature in the dark room for 1 hour. After that, the sections are differentiated in 2% Ferric Chloride for 20 seconds. Wash three times with tap water between each step. The sections are then treated with 5% Sodium Thiosulfate Solution for 1 minute and washed in running tap water for 5 minutes. Next, counterstain in Van Gieson's solution for 3 minutes. Finally, dehydration with 95% and 100% Ethanol, clearing, and then mounting.

## **9. Western blot**

Frozen, normal skin tissue homogenized in RIPA lysis buffer (Thermo Scientific, 89900)



mixed with a protease and phosphatase inhibitor cocktail. Centrifuge at 14,000 rpm for 10 min, and the supernatant was transferred to a new 1.5mL e-tube. The concentration was determined by means of the BCA kit and 2x Laemmli Sample Buffer (BIO-RAD, #1610737) was added, and stored at -20°C.

Proteins were loaded to SDS-PAGE (4–15%) and were separated by their size and transferred to polyvinylidene difluoride membrane (Thermo Scientific). The membranes were blocked with 5% BSA solution and incubated with rabbit anti-mouse collagen I antibody (1:1000, ab34710, Abcam, Cambridge, UK), mouse anti-mouse vimentin antibody (1: 1000, ab8978, Abcam, Cambridge, UK) and mouse anti- $\beta$ -actin (1:5000, sc-47778, Santa Cruz, CA, USA) overnight at 4°C. The membranes were washed three times in PBS with 0.1% Tween 20 prior to 1 hour incubation with secondary antibody of goat anti-mouse IgG-HRP and goat anti-rabbit IgG-HRP (no. A90-116P, A120-101P, Bethyl, Montgomery, TX, USA) at room temperature. Immunoreactive bands were visualized with chemiluminescence using ECL western blot detection reagents (Santa Cruz Biotechnology, Inc.). Data were quantified by band-intensity densitometric analysis (ImageJ).

## **10. Immunohistochemical staining for Vascular Distribution**

For identifying the expression for the CD31 proteins, immunohistochemical staining of the normal skin sections was performed using an automated slide preparation system (Benchmark XT; Ventana Medical Systems Inc., Tucson, AZ, USA). Primary antibody information and incubation time used for staining are listed in **Tables 1** and **2**.

## **11. Statistical analyses**

All data presented as men  $\pm$  standard deviation (SD). Comparisons between multiple groups were performed with the Kruskal–Wallis test, with Prism 8 (GraphPad software, La Jolla, CA,

USA). Step-up Mann–Whitney tests were performed with a multiple comparison adjustment.

\*  $p < 0.05$ , \*\*  $p < 0.01$ , \*\*\*  $p < 0.001$ , \*\*\*\*  $p < 0.0001$ .

**Table 1. The list of antibodies used for Immunohistochemical analysis in this study.**

#	Antibody	Company	Clone	Cat. #
1	Anti-Rabbit CD-68	Abcam	polyclonal	ab125212
2	Anti-Rat Ly6G	Abcam	RB6-8C5	ab25377
3	Anti-Rabbit collagen I	Abcam	polyclonal	ab34710
4	Anti-Rabbit CD31	Abcam	Polyclonal	ab28364

**Table 2. Antibody information used for the Immunohistochemical staining in this study.**

#	Antibody	Company	Dilution	Primary antibody incubation time (min)	Secondary antibody incubation time (min)	Cat. #
1	Anti-CD68	Abcam	1:400	36	16	ab125212
2	Anti-Ly6G	Abcam	1:100	36	16	ab25377
3	Anti-collagen I	Abcam	1:50	36	16	ab34710
4	Anti-CD31	Abcam	1:200	36	32	ab28364

# RESULTS

## 1. Magnetic Resonance Imaging for Volumetric evaluation

HA showed a uniform area of high signal intensity in the early weeks after injection but gradually decreased in intensity over time and was imaged as a heterogeneous area. No difference in signal intensity between the Back and Flank was observed (Figure 1B).

Immediately after injection, the volume of the HA filler was  $155.31 \pm 3.91 \text{ mm}^3$  in the Back and  $162.63 \pm 7.47 \text{ mm}^3$  in the Flank. After 6 weeks of injection, the volume of the HA filler increased to approximately 1.3 to 1.4 times the initial volume. Afterward, the mean volume continued to decrease and week 36 was similar to the initial volume. Flank volume was observed significantly more than Back at all weeks except for weeks 30 and 36 (Figure 1C).

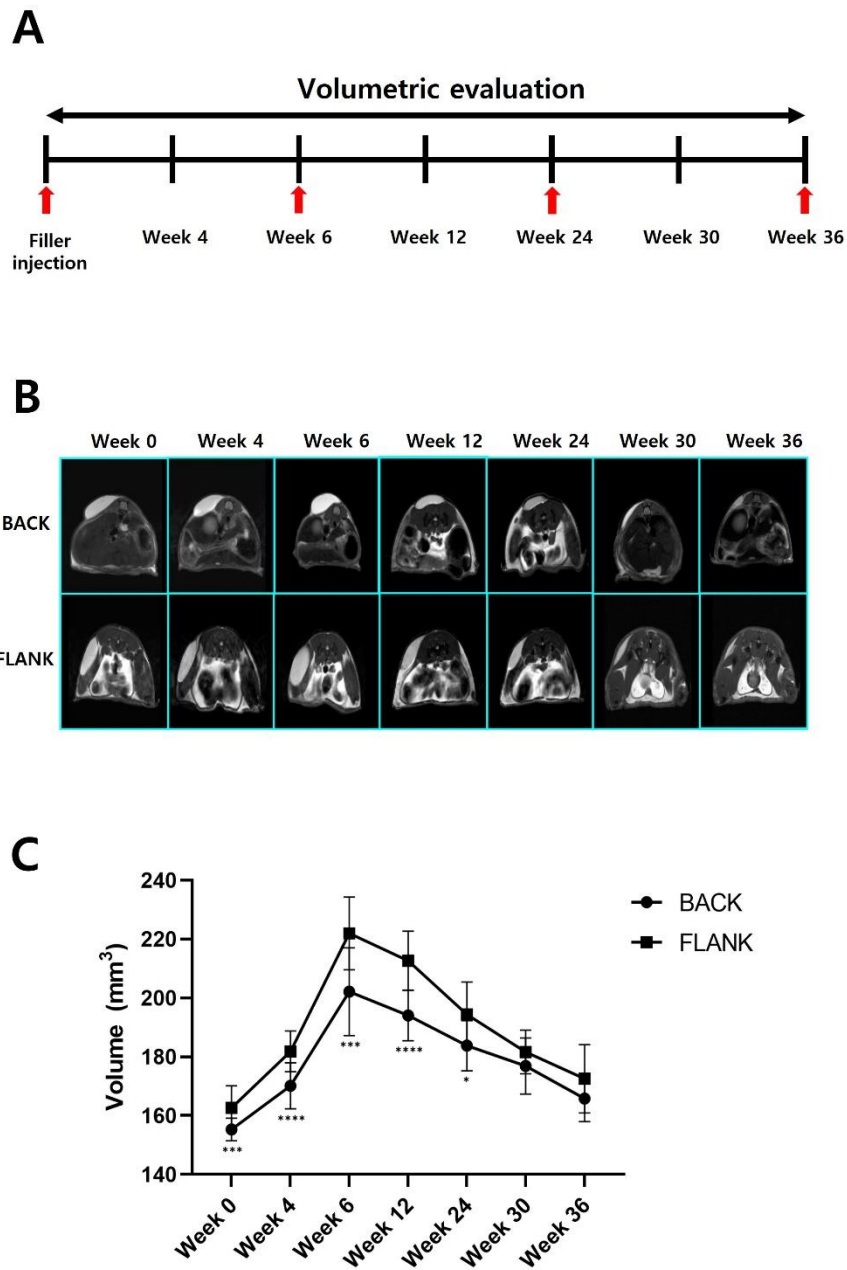


**Figure 1. Volumetric evaluation HA filler *in vivo*.** (A) The schematic represents timeline of data collection (red arrows). (B) Timeline of HA filler morphology and intensity as observed by magnetic resonance imaging. (C) Changes in the volume of HA filler over time as evaluated by magnetic resonance imaging. Data are expressed as mean  $\pm$  standard deviation (SD) of n=6 mice per time. Asterisks indicate significant differences between injection sites at each time point. (\*  $p < 0.05$ , \*\*\*  $p < 0.001$ , \*\*\*\*  $p < 0.0001$ )

## **2. Biocompatibility evaluation through Histopathological examination**

### **2.1 Alcian blue**

The Alcian blue staining image at week 0 shows that the HA filler was injected as a mass subcutaneously between the skin and muscle layer. The density of HA filler at week 6 was higher than that at week 0, and blue-stain staining was more intense. Then, at weeks 24 and 36, it was observed that the degradation of HA gradually progressed, the density was lowered, and the staining faded. No difference in biodegradability between the Back and Flank was observed on Alcian blue staining (Figure 2).

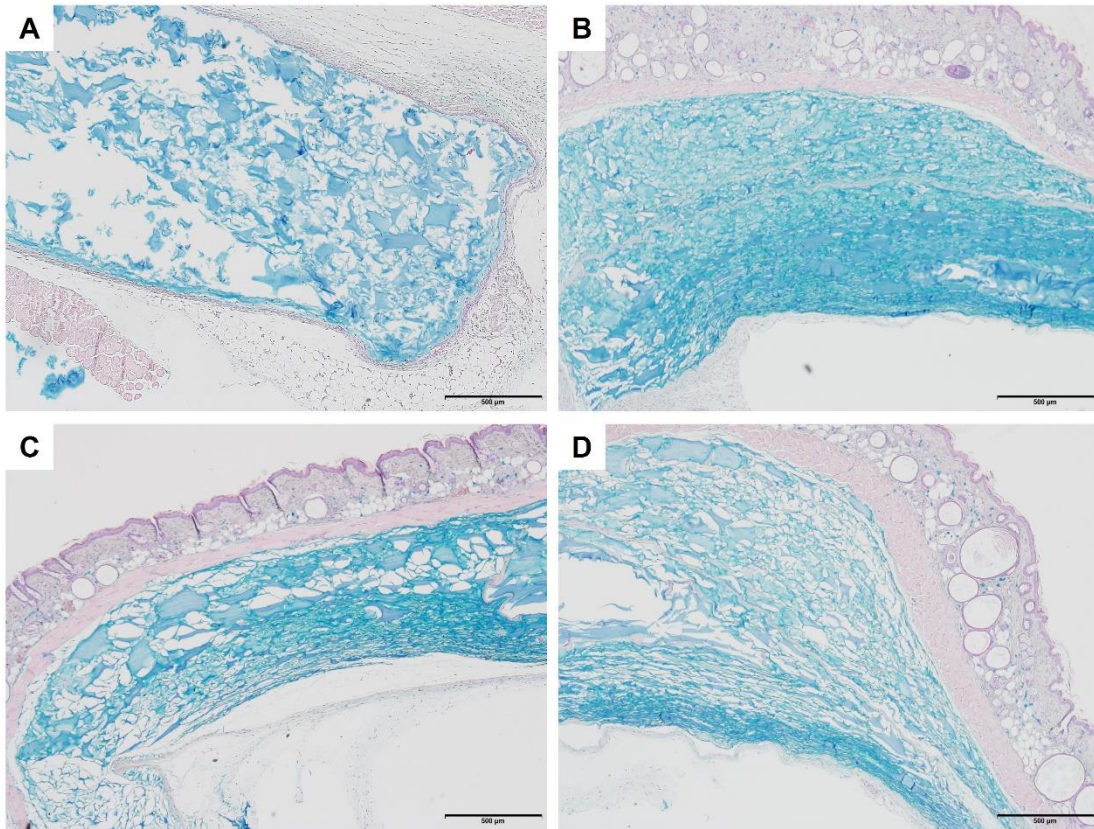


**Figure 2. Evaluation of biodegradability of HA filler using Alcian blue. Blue-stained area represented HA in subcutaneous. Scale bars = 500μm.**

## **2.2 Hematoxylin and eosin**

Histopathological examination of skin (injection sites) tissue was conducted using all the Hematoxylin and Eosin-stained slides. On histopathological examination of H&E stained skin (injection sites) tissue, HA filler was observed as basophilic amorphous materials in the subcutaneous tissue under the panniculus muscle. It remained in the same location at weeks 6, 24, and 36. However, it was observed that the area of the encapsulated amorphous materials decreased over time.

In the case of the inflammatory reaction, it was observed that at week 0, minimal inflammatory cell infiltration with histiocytes was scattered around the HA (Figure 3B). Histiocytes were still observed at 6 (Figure 3C) weeks but significantly decreased compared to week 0 and were hardly observed at weeks 24 and 36. Compared to week 0, the fascial fibrous capsule began to form with 2-3 layers from week 6 and was observed as a single thick layer at weeks 24 and 36. No significant differences between the Back and Flank were observed.



### **2.3 Immunohistochemical staining for CD 68 and Ly6g**

Immunohistochemical staining of CD68 and Ly6g was performed to evaluate and compare tissue reactions after subcutaneous injection of HA fillers. The immunohistochemical staining results comprehensively assess the intensity and frequency of specific positive staining for each antibody, designate 8 areas at X200 magnification, and then quantitatively measure the ratio of the positively stained cell area to the total area using QuPath v0.3.0. was scored.

In the case of CD68, the highest proportion of positively stained cells was observed in the Back and Flank area at  $31.48 \pm 5.61$  % and  $36.51 \pm 10.43$  %, respectively, at week 0 after injection. The proportion gradually decreased over time and was observed to be  $4.38 \pm 0.81$  % and  $5.02 \pm 0.54$  % at week 36 (Figure 3D).

In the case of Ly6g, the highest proportion of positively stained cells was observed in the Back and Flank area at  $4.84 \pm 1.63$  % and  $5.05 \pm 1.72$  %, respectively, at week 0 after injection. The proportion gradually decreased over time and was almost not observed at 36 weeks (Figure 3E).

No significant difference in tissue reactions between the Back and Flank areas as analyzed by immunohistochemical staining.

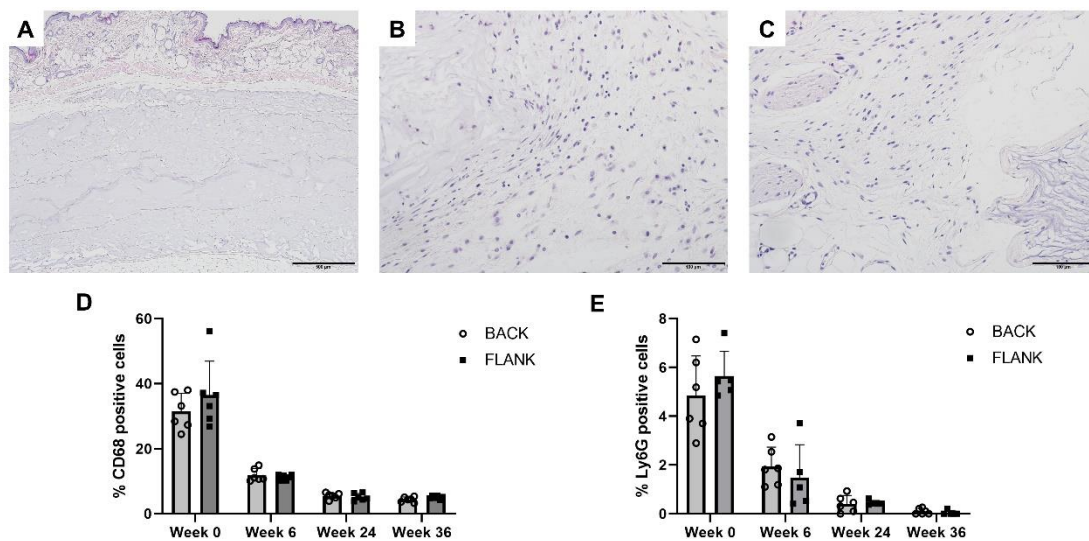


**Figure 3. Inflammatory reaction over time after injection of HA.** (A) Basophilic amorphous material. *Scale bars* = 500  $\mu$ m (B) At week 0 of HA injection, histiocytes and neutrophils. (C) At the week 6 of HA injection, histocyte. *Scale bars* = 100  $\mu$ m. (D) Histocyte activation was assessed by determining CD68 positive cells by immunohistochemistry (IHC). (E) Neutrophil activation was assessed by determining Ly6G positive cells by IHC. Data are expressed as mean  $\pm$  standard deviation (SD) of n=6 mice per time. No significant difference between the Back and Flank.

### **3. Collagen synthesis**

#### **3.1 Masson's Trichrome and Sirius Red**

To evaluate the synthesized collagen after HA filler injection, analysis of capsule thickness and collagen content was performed following Masson's trichrome and Sirius red staining. Collagen fibers were stained blue in Masson's trichrome and red in Sirius red, and the areas were extracted and measured for capsule thickness and collagen area using Image J.

Capsule thickness was measured and compared from the 8 regions of the random image. Capsule formation around the HA filler was observed week 6 after injection, and the thickness gradually diminished over time, but no significant changes were observed. When comparing the injection sites, the capsule thickness was thicker in the Flank area where the filler was injected compared to the Back in all weeks. Except for week 0, significant differences were observed in the fibrous capsule thickness at every week.

Collagen content was compared by calculating the ratio of the area stained blue (Masson's trichrome) or red (Sirius red) to the total area after designating eight ROIs. The percentage of positively stained area significantly increased from the week 6 and gradually decreased after that. Similarly, in all weeks, the ratio of the positively stained area was higher in the Flank area where the filler was injected than in the Back. There was statistical significance between the Back and Flank in every week.

### **3.2 Immunohistochemical staining for collagen I**

The amount of collagen I expression was compared by designating 8 ROIs and calculating the ratio of the number of positive cells to the total area. Immunohistochemical studies showed that collagen I protein appeared the most abundantly at week 6 with  $55.96 \pm 12.92$  % in the Back and  $79.41 \pm 12.52$  % in the Flank, and gradually decreased after that. Statistically significantly collagen I was more expressed in Flank than Back at every time point (Figure C, H).

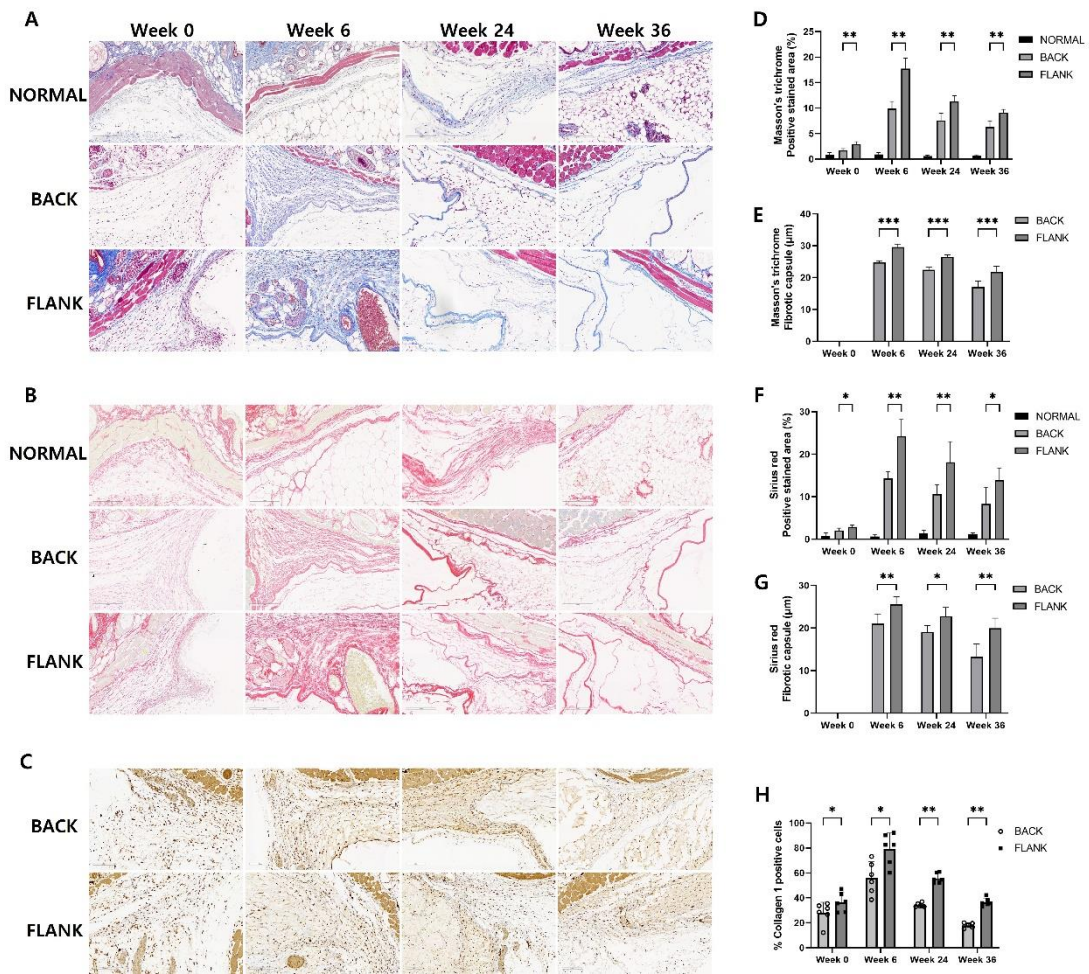


**Figure 4. Collagen staining with histochemical and IHC.** (A) Blue-stained area represented collagen of the subcutaneous. Original magnification, 200X. (B) Red-stained area represented collagen of the subcutaneous. (C) Collagen I activation was assessed by determining collagen I positive cells by IHC. (D, F) The quantitative analysis on proportion of positive stained area. (E, G) The thickness analysis of fibrotic capsule. (H) The quantitative analysis of collagen I-positive cells. Data are expressed as mean  $\pm$  standard deviation (SD) of  $n=6$  mice per time. Asterisks indicate significant differences between injection sites at each time point. (\*  $p < 0.05$ , \*\*  $p < 0.01$ , \*\*\*  $p < 0.001$ )

#### **4. Elastic fiber**

In Verhoeff van Gieson staining, elastic fibers were stained black, and positively stained elastic fibers showed an elongated shape and were observed in the dermis. No increase or decrease in elastic fiber over time was observed when HA was injected subcutaneously, and no differences were observed between Back and Flank at all weeks (Figure 5).

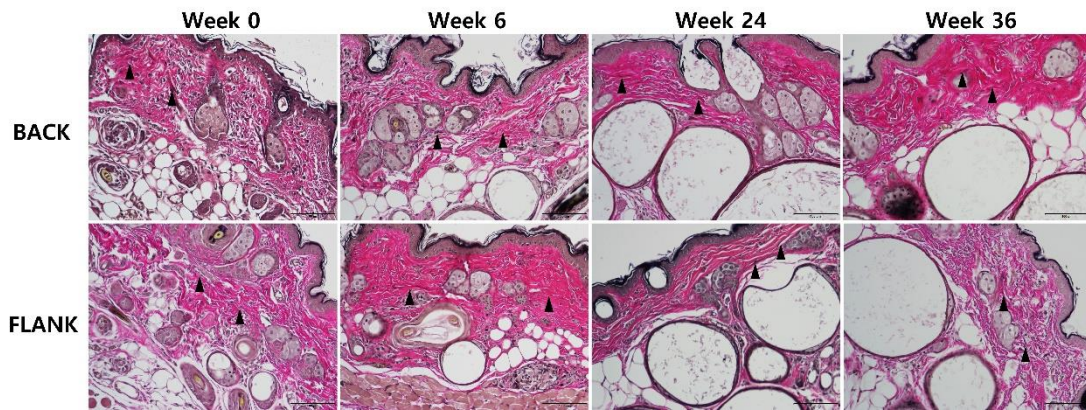


**Figure 5. Elastic fiber staining with Verhoeff van Gieson. Black-stained area represented elastic fiber of the dermis. *Scale bars* = 100  $\mu$ m**

## **5. Collagen synthesis microenvironment**

### **5.1 Western blot**

The amount of protein related to fibroblast differentiation was measured in the Back and Flank of normal skin tissue to analyze the difference in the collagen synthesis microenvironment according to the anatomical area. As proteins, vimentin, an intracellular marker of fibroblasts, and collagen I, a secreted marker, were selected.

As a result, collagen I (120kDa) and vimentin (53kDa) were significantly expressed in the Flank than in the Back of normal skin tissue. Anti- $\beta$ -actin was also measured to confirm that the amount of loaded sample was constant. The relative collagen I and vimentin levels were normalized to anti- $\beta$ -actin (Figure 6).



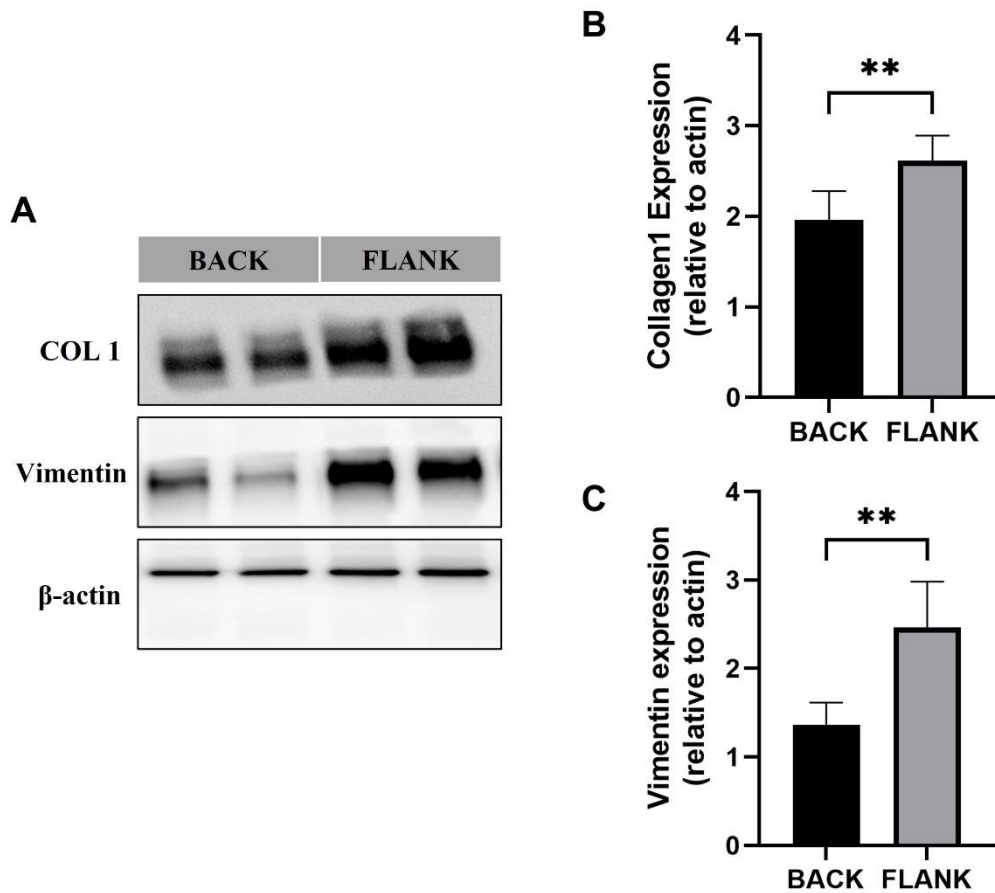


**Figure 6. Evaluation of fibroblast differentiation with Western blot.** (A) Protein obtained from normal skin tissue. Two representative bands were detected (120kDa and 53kDa).  $\beta$ -actin Western blot was performed at the same time. (B) The expression levels of collagen I. (C) The expression levels of Vimentin. Data are expressed as mean  $\pm$  standard deviation (SD) of n=8 mice per group. Asterisks indicate significant differences between injection sites. (\*\*  $p < 0.01$ )

## **5.2 Immunohistochemical staining for CD31**

CD31 IHC staining was performed on the Back and Flank of normal skin tissue slides to analyze differences in vascular distribution among microenvironmental factors that affect collagen synthesis according to anatomical regions.

The amount of CD31 expression was compared by designating 8 ROIs and calculating the ratio of the area of positively stained cells to the total area. Immunohistochemical studies showed that statistically significantly CD31 protein was more expressed in the Flank than the Back (Figure 7B).

Subcutaneous fat thickness was the average measured by designating 8 ROIs. Similar to vascular distribution, subcutaneous fat thickness was also observed to be about 4.3 times thicker in the Flank. (Figure 7C).

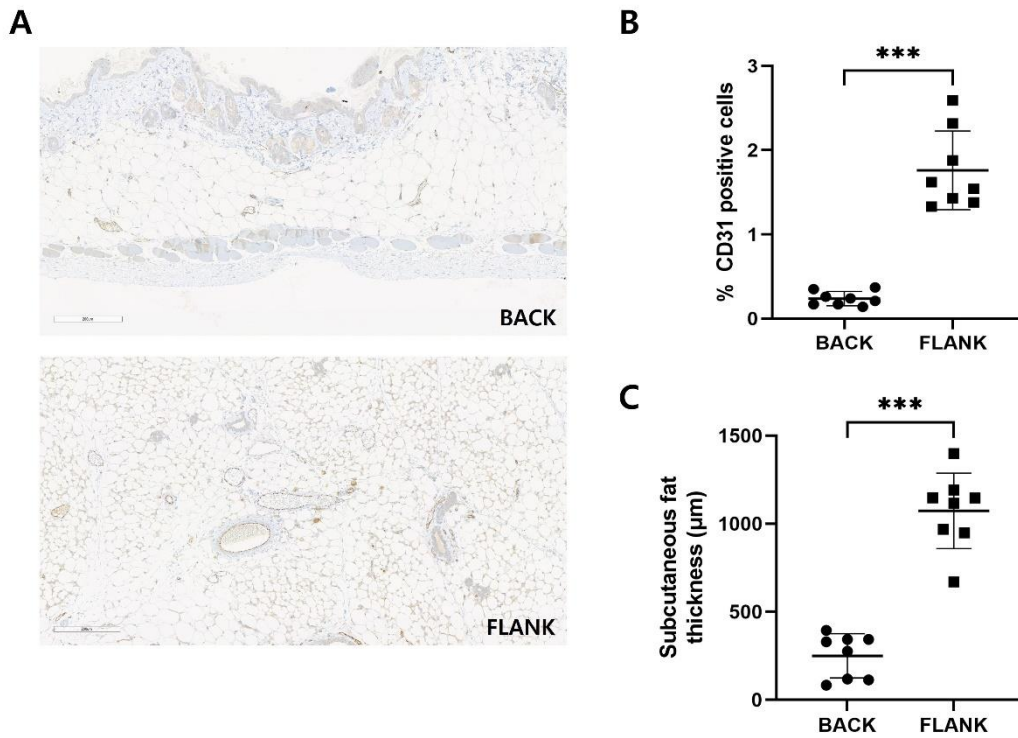


**Figure 7. Evaluation of vascular distribution and subcutaneous fat thickness.** (A) Representative images of immunohistochemical staining for CD31. Original magnification, 200X. (B) Vascular density was assessed by determining CD31 positive cells by IHC. (C) Subcutaneous fat thickness was assessed. Data are expressed as mean  $\pm$  standard deviation (SD) of  $n=8$  mice per group. Asterisks indicate significant differences between injection sites. (\*\*\*)  $p < 0.001$ )

## DISCUSSION

In this study, the Back and Flank of the mouse were selected as representative areas of “eyelid” and “nasal tip” in clinical based on skin thickness. Histological examination was performed to evaluate the biocompatibility of filler and differences in collagen synthesis between anatomical injection sites. In addition, differences in the collagen synthesis microenvironment between anatomical injection sites were compared to evaluate the suitability of the anatomical structure of the injection site according to the type of filler when introducing a new filler product for clinical use.

As a result of *in vivo* volumetric measurement through MRI by injecting hyaluronic acid (HA) filler to the Back and Flank of the mouse, the volume increase by HA injection occurred more in the Flank and the volume increased until the week 6 and then decreased.

HA fillers' degradation rate depends on the concentration of HA and cross-linking agents such as 1,4-butanediol diglycidyl ether (BDDE) and cross-linking degree [19]. The half-life of naturally occurring HA is less than 3 days, and the polymer's molecular weight and degree of cross-linking are controlled to prolong the degradation time [20]. HA cross-linking provides a chemical barrier against degradation by hyaluronidase and is important for generating longer-lasting HA-based hydrogels. The initial concentration of HA plays a crucial role in determining the cross-linking efficiency of BDDE-crosslinked HA hydrogels. The swelling ability of the hydrogel decreased steadily up to 10.0% HA hydrogel as the initial concentration increased, then showed the opposite trend. Low HA hydrogels have weak scaffolds and large pores, so more water is absorbed into the hydrogel matrix and causes greater swelling [21]. Since the swollen gel network subsequently decreases in size through degradation and exposure to hyaluronidase, the swelling ratio depending on HA's initial concentration may affect the HA filler's degradation rate [22]. It has also been reported that the swelling rate of the mono-phasic filler is faster than that of the bi-phasic filler, and the degree of swelling is

more pronounced [1].

Therefore, in this study, when mono-phasic filler cross-linked with BDDE was injected, the swelling effect occurred up to week 6. And then, it gradually decreased due to enzymatic degradation within the swollen gel network, and at week 36, it was measured similarly to the initial injection volume. The duration of these effects has been reported to range from 3 to 6 months depending on the specific injection site, and it can be seen as a clearance action by the breakdown of cross-links.

Through the result of IHC and histochemical staining, it was confirmed that HA was encapsulated, degraded by macrophages, and replaced with collagen fibers. The accumulation of collagen fibers occurred more in the Flank. HA itself stimulates migration and proliferation of fibroblasts by activating CD44 and CD168, which are hyaluronan receptors expressed on cell membranes [23-25]. An increase in extracellular matrix components such as collagen, elastin, and proteoglycan has been reported as a result of activated fibroblasts, which provide stability by creating a lattice structure [26, 27]. The observed encapsulation, degradation by macrophages, and subsequent replacement by fibrous tissue are the reasons why dermal volume at the injected site may remain despite reabsorption of the material. In addition, this is a characteristic of biocompatible materials for relieving inflammatory reactions [28].

Biocompatibility is a key property of products used as dermal filler materials, traditionally defined as no or little tissue response to an implant material [15]. Some complications such as acute or chronic inflammation due to filler injection may occur in a small number of patients, so medical devices used by humans require biocompatibility evaluation to prevent damage or injury to the host [29]. As a result of histopathological examination, minimal inflammatory cells were observed at week 0 of injection and gradually decreased thereafter. This is a minimal tissue reactivity and local inflammatory response with injection, suggesting that HA filler is stable [28].

Differences in collagen synthesis microenvironments were compared by observing differences in collagen synthesis according to anatomical injection sites. As a result of Western blotting, high levels of vimentin and collagen I expression was observed in the Flank, indicating active differentiation of fibroblasts essential for collagen formation [30]. Challa, A.A. and B (2011) observed that disruption of vimentin reduced the synthesis of type I collagen, a major component of the extracellular matrix in fibrotic tissue [31]. Cheng, Fet al. (2016) observed no collagen accumulation in vimentin-deficient wounds, which is a direct result of severe inhibition of fibroblast proliferation and expansion [32]. The results of two studies suggest that vimentin is necessary for the proliferation of fibroblasts responsible for collagen production and secretion. Therefore, the results of this study indicated that fibroblasts are more active in the Flank than the Back.

Collagen synthesis is a complex process involving various factors, including the availability of nutrients and oxygen [33]. Blood vessels provide these essential elements to the fibroblasts responsible for collagen production. The vascular distribution can vary greatly across anatomical regions and is expected to lead to differences in collagen synthesis. As a result of performing CD31 IHC staining on normal skin tissues, it was confirmed that the blood vessel density was high in the Flank, which had a high collagen expression level. This result suggests that the distribution of blood vessels is one of the factors affecting the level of collagen synthesis. However, only a few studies have been conducted on the relationship between vascular distribution and collagen synthesis, so that can limit the generalizability of the findings. Examining the relationship between vascular distribution and collagen synthesis in various tissues and disease states would have provided further insight into the underlying mechanisms.

This study tried to evaluate the suitability of the anatomical structure of the injection site according to the type of filler. The purpose of improving skin texture should be injected into

the dermis, and the reason for volumizing should be injected into subcutaneous [34]. Therefore, in subcutaneous injection studies aimed at reducing wrinkles by adding volume, it was not appropriate to observe changes in elastic fibers indicating improved elasticity.

In this study, biocompatibility was evaluated using various evaluation methods such as radiology (MRI) and molecular biology (Western blot) as well as histological examination of filler injection. In addition, it provided insight into clinical use by selecting an anatomical site in consideration of the site suitable for the purpose of the filler and comparing the difference. In this study, the difference between Back and Flank was studied, but future research could be able to apply to various anatomical sites considering the relationship between animals and humans in context of physiology and the intended use of fillers. Therefore, it will be able to provide information for selecting the anatomical injection site of animal study for more complete preclinical studies.

## REFERENCES

1. Ryu, H.-j., et al., Model-based prediction to evaluate residence time of hyaluronic acid based dermal fillers. *Pharmaceutics*, 2021. **13**(2): p. 133.
2. Chen, W.J., Functions of hyaluronan in wound repair. *Hyaluronan*, 2002: p. 147-156.
3. Toole, B.P. Hyaluronan in morphogenesis. in *Seminars in cell & developmental biology*. 2001. Elsevier.
4. Ghosh, K., Biocompatibility of hyaluronic acid: From cell recognition to therapeutic applications, in *Natural-Based Polymers for Biomedical Applications*. 2008, Elsevier. p. 716-737.
5. Flynn, T.C., et al., Comparative histology of intradermal implantation of mono and biphasic hyaluronic acid fillers. *Dermatologic surgery*, 2011. **37**(5): p. 637-643.
6. Kim, M., et al., Ex vivo magnetic resonance imaging using hyaluronic acid fillers: Differences between monophasic and biphasic fillers. *Skin Research and Technology*, 2018. **24**(1): p. 16-19.
7. Hillel, A.T., et al., Validation of a small animal model for soft tissue filler characterization. *Dermatologic surgery*, 2012. **38**(3): p. 471-478.
8. Fan, Y., et al., Hyaluronic acid-cross-linked filler stimulates collagen type 1 and elastic fiber synthesis in skin through the TGF- $\beta$ /Smad signaling pathway in a nude mouse model. *Journal of Plastic, Reconstructive & Aesthetic Surgery*, 2019. **72**(8): p. 1355-1362.
9. Quan, T. and G.J. Fisher, Role of age-associated alterations of the dermal extracellular matrix microenvironment in human skin aging: a mini-review. *Gerontology*, 2015. **61**(5): p. 427-434.
10. Quan, T., et al., Enhancing structural support of the dermal microenvironment activates fibroblasts, endothelial cells, and keratinocytes in aged human skin *in vivo*. *Journal of Investigative Dermatology*, 2013. **133**(3): p. 658-667.
11. Hata, A. and Y.-G. Chen, TGF- $\beta$  signaling from receptors to Smads. *Cold Spring Harbor perspectives in biology*, 2016. **8**(9): p. a022061.
12. Zhang, L., F. Zhou, and P. ten Dijke, Signaling interplay between transforming growth factor- $\beta$  receptor and PI3K/AKT pathways in cancer. *Trends in biochemical sciences*, 2013. **38**(12): p. 612-620.
13. Kim, J.-E. and J.M. Sykes, Hyaluronic acid fillers: history and overview. *Facial Plastic Surgery*, 2011. **27**(06): p. 523-528.
14. Lemperle, G., V. Morhenn, and U. Charrier, Human histology and persistence of various injectable filler substances for soft tissue augmentation. *Aesthetic plastic surgery*, 2003. **27**: p. 354-366.



15. Fernández-Cossío, S. and M.T. Castaño-Oreja, Biocompatibility of two novel dermal fillers: histological evaluation of implants of a hyaluronic acid filler and a polyacrylamide filler. *Plastic and reconstructive surgery*, 2006. **117**(6): p. 1789-1796.
16. Anderson, J.M., Mechanisms of inflammation and infection with implanted devices. *Cardiovascular Pathology*, 1993. **2**(3): p. 33-41.
17. Greene, J.J. and D.M. Sidle, The hyaluronic acid fillers: current understanding of the tissue device interface. *Facial Plastic Surgery Clinics*, 2015. **23**(4): p. 423-432.
18. Lee, W., et al., Clinical application of a new hyaluronic acid filler based on its rheological properties and the anatomical site of injection. *Biomedical Dermatology*, 2018. **2**: p. 1-5.
19. Keizers, P.H., et al., A high crosslinking grade of hyaluronic acid found in a dermal filler causing adverse effects. *Journal of Pharmaceutical and Biomedical Analysis*, 2018. **159**: p. 173-178.
20. Lee, W., et al., Practical guidelines for hyaluronic acid soft-tissue filler use in facial rejuvenation. *Dermatologic Surgery*, 2020. **46**(1): p. 41-49.
21. Al-Sibani, M., A. Al-Harrasi, and R. Neubert, Effect of hyaluronic acid initial concentration on cross-linking efficiency of hyaluronic acid-based hydrogels used in biomedical and cosmetic applications. *Die Pharmazie-An International Journal of Pharmaceutical Sciences*, 2017. **72**(2): p. 81-86.
22. Park, S., et al., Investigation of the degradation-retarding effect caused by the low swelling capacity of a novel hyaluronic acid filler developed by solid-phase crosslinking technology. *Annals of Dermatology*, 2014. **26**(3): p. 357-362.
23. Fraser, J.R.E., T.C. Laurent, and U. Laurent, Hyaluronan: its nature, distribution, functions and turnover. *Journal of internal medicine*, 1997. **242**(1): p. 27-33.
24. Mast, B.A., et al., Hyaluronic acid modulates proliferation, collagen and protein synthesis of cultured fetal fibroblasts. *Matrix*, 1993. **13**(6): p. 441-446.
25. Greco, R.M., J.A. Iacono, and H.P. Ehrlich, Hyaluronic acid stimulates human fibroblast proliferation within a collagen matrix. *Journal of cellular physiology*, 1998. **177**(3): p. 465-473.
26. Paliwal, S., et al., Skin extracellular matrix stimulation following injection of a hyaluronic acid-based dermal filler in a rat model. *Plastic and reconstructive surgery*, 2014. **134**(6): p. 1224-1233.
27. Mochizuki, M., et al., Evaluation of the *in vivo* kinetics and biostimulatory effects of subcutaneously injected hyaluronic acid filler. *Plastic and Reconstructive Surgery*, 2018. **142**(1): p. 112-121.
28. Anees, M.M., R.H. Al-Serwi, and A.S. Abd Elhamied, BIOCOMPATIBILITY OF HYALURONIC ACID FILLER IN CHEEK MUCOSA (EXPERIMENTAL STUDY).
29. Cannella, V., et al., In vitro biocompatibility evaluation of nine dermal fillers on L929

- cell line. BioMed Research International, 2020. **2020**.
30. Walker, J., et al., In wound repair vimentin mediates the transition of mesenchymal leader cells to a myofibroblast phenotype. *Molecular biology of the cell*, 2018. **29**(13): p. 1555-1570.
  31. Challa, A.A. and B. Stefanovic, A novel role of vimentin filaments: binding and stabilization of collagen mRNAs. *Molecular and cellular biology*, 2011. **31**(18): p. 3773-3789.
  32. Cheng, F., et al., Vimentin coordinates fibroblast proliferation and keratinocyte differentiation in wound healing via TGF- $\beta$ -Slug signaling. *Proceedings of the National Academy of Sciences*, 2016. **113**(30): p. E4320-E4327.
  33. Palmieri, B., M. Vadalà, and C. Laurino, Nutrition in wound healing: investigation of the molecular mechanisms, a narrative review. *Journal of Wound Care*, 2019. **28**(10): p. 683-693.
  34. Kim, J., Effects of Injection Depth and Volume of Stabilized Hyaluronic Acid in Human Dermis on Skin Texture, Hydration, and Thickness. *Archives of Aesthetic Plastic Surgery*, 2014. **20**(2): p. 97-103.

## 국문요약

### 히알루론산 투여 부위의 해부학적 차이에 따른 필러의 생체적합성 비교 연구

히알루론산은 D-글루루론산과 N-아세틸 글루코사민의 반복 이당류 단위로 구성된 음이온 글리코사미노글리칸으로 조직 부피와 수분 공급을 제공하는 살아있는 유기체의 천연 고분자입니다. 히알루론산은 조직 복구, 형태 형성, 세포 증식 및 이동과 같은 다양한 생리학적 과정에서 중요한 역할을 합니다. 히알루론산은 조직 합성 및 매트릭스 리모델링을 촉진하여 조직 부피를 제공하고 피부를 보호하는 점탄성 세포내 매트릭스의 중요한 구성 요소가 됩니다. 물 분자를 결합하고 유지하는 능력은 피부 필러에 사용될 때 조직의 수분을 유지하고 매끄럽고 자연스러운 외관에 기여합니다.

섬유아세포와 세포외기질(ECM) 사이의 상호 작용은 세포 기능에 매우 중요합니다. 가교된 HA 투여가 섬유아세포 증식을 유도하여 I형 콜라겐을 자극한다는 여러 연구 결과가 보고되었으며, 섬유아세포의 활성 능력을 조절하는 ECM 미세 환경의 중요성이 강조되어 왔습니다. 콜라겐은 조직에 힘과 지지를 제공하는 주요 구조 단백질입니다. 섬유아세포에 의한 콜라겐 합성은 Smad 전사 인자와 같은 다운스트림 이펙터 단백질을 활성화시키는 TGF- $\beta$  (transforming growth factor-beta) 경로에 의해 조절됩니다. TGF- $\beta$ 는 MAPK 및 PI3K/AKT 경로를 활성화하여 콜라겐 합성에 기여할 수 있습니다.

더말 필러의 생체적합성은 숙주 조직 반응과 이식된 물질의 특성에 영향을 받기 때문에 매우 중요하며, 이러한 상호 작용은 필러의 장기적인 효능과 안전성을

손상시킬 수 있는 반응을 유도합니다. 따라서 투여 물질에 대한 조직 반응을 평가하고 안전성과 효능을 보장하려면 적절한 조직학적 평가가 필요합니다.

히알루론산 필러를 포함한 더말 필러는 잔주름 교정, 얼굴 볼륨 증가, 피부 질 개선을 위한 심미적 회춘에 사용되며 목적에 맞는 해부학적 부위에 적용됩니다. 필러 주입을 위한 해부학적 부위의 선택은 주입할 피부 층과 해당 부위의 피부 두께를 고려해야 합니다. 그러나 해부학적 부위에 초점을 맞춘 생체 적합성 연구는 아직까지 연구되지 않았습니다.

본 연구에서는 피부 두께를 기준으로 임상에서 눈꺼풀과 코끝의 대표적인 부위로 마우스의 등(Back) 및 옆구리(Flank)를 선정하였습니다. 필러의 생체적합성과 해부학적 주사 부위에 따른 콜라겐 합성의 차이를 평가하기 위해 조직학적 검사를 수행하였습니다. 이후 해부학적 투여 부위 간의 콜라겐 합성 미세환경 차이를 비교하여 새로운 필러 제품을 임상에 도입할 때 필러 종류에 따른 투여 부위의 해부학적 구조의 적합성을 평가하였습니다.

MRI 이미지 분석 결과, 히알루론산 투여에 의한 볼륨 증가는 Flank에서 더 많이 발생하는 것을 관찰하였으며 면역조직화학염색(IHC), Masson's trichrome 및 Sirius red 염색을 통해 Flank에서 콜라겐 합성이 더 잘 일어나는 것을 관찰하였습니다. 또한 콜라겐 합성 미세환경 차이를 평가하기 위해 수행한 Western blot 및 CD31 IHC를 통해 Flank에서 피하지방이 많고 혈관이 많이 분포되어 있으며 섬유아세포가 활발하게 분화된 것을 관찰하였습니다. 따라서 히알루론산 투여에 의한 볼륨 증가 및 콜라겐 합성은 피하지방과 섬유아세포가 많은 Flank에서 더 잘 일어났습니다.

본 연구에서는 필러 투여의 조직학적 검사뿐만 아니라 영상의학(MRI) 및 분자생물학(Western blot)과 같은 다양한 평가 방식을 사용하여 생체적합성을 평가하

였습니다. 또한 필러의 목적에 맞는 부위를 고려하여 해부학적 부위를 선정하고 차이를 비교함으로써 임상적 사용에 대한 통찰력을 제공하였습니다.

**중심단어:** Hyaluronic acid (HA); Collagen synthesis; ECM microenvironment; Biocompatibility; Anatomical injection site